Lifelong temporal dynamics of the gut microbiome associated with longevity in mice

Lena Takayasu[1, 2], Eiichiro Watanabe[2], Taichi Umeyama[2], Rina Kurokawa[2,3], Yusuke Ogata[2], Yuya Kiguchi[2,3], Hiroaki Masuoka[2], Masahiro Umezaki[1], Masahira Hattori*[2, 3], and Wataru Suda*[2]

[1] Department of Human ecology, Graduate School of Medicine, The University of Tokyo. 7-3-1, Hongo, Bunkyo-ku, Tokyo 113-0033 Japan

[2] Laboratory for Microbiome Sciences, IMS, RIKEN. 1-7-22 Suehiro-cho Tsurumi-ku, Yokohama, Kanagawa 230-0045 Japan

[3] Cooperative Major in Advanced Health Science, Graduate School of Advanced Science and Engineering, Waseda University. 3-4-1 Okubo Shinjuku-ku, Tokyo 169-8555 Japan

* Corresponding authors:
Wataru Suda
Tel.: +81-45-503-9302
E-mail: wataru.suda@riken.jp

Abstract

The effect of lifelong dynamics on host longevity of the gut microbiome is largely unknown. Herein, we analyzed the longitudinal fecal samples of seven sibling mice across their lifespan from birth to natural death, spanning over 1,000 days of age, and maintained them under controlled environmental and dietary conditions. Our 16S-rRNA sequencing analysis revealed 38 common "life-core" bacterial species/OTUs (operational taxonomic units) detected in ≥80% of all samples collected across the lifespan of individual mice. Despite the shared genetic background and dietary habits, the gut microbiome structure significantly diversified with age and among individuals. We found a strong positive correlation between longevity and the alpha diversity in middle age (500-700 days) and negative correlation in old age (>800 days). Furthermore, host longevity was significantly associated with the abundance of 17 bacterial species/OTUs, most of which were "life-core" species. Our data suggest that temporal dynamics of the gut microbiome are strongly linked to host longevity.

Introduction

It has long been hypothesized that the gut microbiome affects the longevity and aging of hosts. In studies using germ-free animals show longer lifespans than conventional animals[1], and the administration of antibiotics in mice and insects extends the lifespan of mice[2,3]. In addition to sterilization, fecal microbiota transplantation from wild-type mice into progeroid mice has been reported to enhance both the health and lifespan of mice[4]. Moreover, the administration of the probiotic bacterium Bifidobacterium animalis or Akkermansia muciniphila has been shown to extend the lifespan of mice[4-6]. Low-calorie diets are also associated with a prolonged life span in many biological species[7–9], including worms, flies, mice, and rats, and the underlying mechanism of this effect was recently reported to be associated with the gut microbiome[10]. These studies directly suggest that the gut microbiome is involved in the prolongation of lifespan; however, it remains unclear how structural variations in the gut microbiome play a role in the prolongation of lifespan.

In the last decade, culture-independent metagenomics with advanced sequencing technologies have allowed the investigation of differences in the structure of the gut microbiome at different life stages, from infancy to the elderly[11–18]. Most of these metagenome-based human cohort studies have shown covariance of age with the gut microbiome by comparing gut microbiomes between different age groups. However, these approaches do not accurately determine whether the age-associated differences in gut microbiomes are primarily associated with chronological age or confounded by other factors such as lifestyles because individuals in different age groups might have been exposed to different environmental and lifestyle events. In addition, patient history, including medications and a history of gut microbial colonization, may also affect the gut microbiome of humans throughout life. In contrast, mice have a lifetime of two-three years, enabling the monitoring of time

series variations in the gut microbiome over a lifetime. Therefore, the present study aimed to clarify the intimate transition in the gut microbiome with age using mice instead of humans. We analyzed fecal samples longitudinally collected from siblings of specific pathogen-free (SPF) mice throughout their whole life from birth to death, spanning more than 1,000 days, to elucidate the association of gut microbiomes with the lifespan of hosts and life events, including pregnancy, delivery, and cohousing, under the same rearing environments.

Results

Mice, collection of fecal samples, and 16S rRNA gene analysis. We purchased and bred the parent mice (Mo and Fa, SPF C57BL/6J strain), which thereafter had nonuplet mice (one male, seven females, and one unknown) at the animal facility. Of these siblings, seven mice (M1, 2, 3, 4, 5, 7, and 8) died of natural causes with a mean lifetime of 922.7 ± 71.6 days ranging from 827 to 1,044 days, one mouse (M6) died with a shorter lifespan than the others at 524 days probably due to the development of a tumor under the same controlled environmental, and one mouse (M9) died immediately after birth.

Throughout the experiment, the eight siblings were cohoused with their parents for 51 days after birth, and thereafter cohoused with different combinations of individuals in different cages, and three (M3, M7, and M8) and Mo experienced pregnancy and delivery (Table S1). We performed immediate autopsies of the dead mice and observed tumors in five mice (M2, 6, 7, 8, and Mo) but not in others (M1, 3, 4, 5, and Fa).

We longitudinally collected a total of 1,815 fecal samples from 10 mice (eight siblings and parents) with an average sampling interval of 4.3 days and obtained a total of 18.0 million high-quality reads of the 16S rRNA gene V1-2 region from fecal DNA samples using the Illumina MiSeq platform (Table S1, Methods). Clustering of 16S reads from samples of the seven siblings with natural death with 97% identity individually generated operational taxonomic units (OTUs) ranging from 4,094 to 6,984 OTUs (5,646 OTUs on average), of which 11 to 17% (13% on average) were OTUs with ≥0.1% abundance in at least one sample of each mouse. In addition, clustering of 16S reads from all samples of the 10 mice (eight siblings and parents) generated a total of 21,768 OTUs, including 6,531 OTUs with ≥0.1% abundance in at least one sample, which was used for analysis with common OTU IDs in this study (Table S1).

Temporal variations in α-diversity across a lifetime. Analysis of the cumulative number of OTUs with ≥0.1% abundance in at least one sample over a lifetime of 200 days after birth revealed that over 50 and 90% of the total OTUs appeared within 28 and 167 days in the samples of the seven siblings, respectively (Extended Data Fig. 1). The number of OTUs rapidly increased to 200–300 in the first 20 days, although 9–15 OTUs were detected in 0-day samples of four mice (M2, 3, 6, and 8), and were relatively constant after 100 days in most mice (Extended Data Fig. 2). The number of OTUs in the

bins of four mice (M3, 5, 7, and 8) was relatively constant across the lifetime after 100 days compared to that of the others (M1, 2, and 4), which tended to have a lower number of OTUs in the latter half of the lifespan of mice. We observed an increase in the number of OTUs in the last two bins just before death in six out of seven mice, and four of them were significantly increased (Student's t-test, P <0.05).

Temporal variations in β-diversity across a lifetime. The principal coordinate analysis (PCoA) of weighted and unweighted UniFrac distances of all samples across the lifetime of the seven siblings revealed that the most prominent difference in β-diversity across samples was that in samples before and after 20 days (Figs. 1A and B), consistent with the change in the number of OTUs in the early lifetime shown in Extended Data Fig. 2. The data also showed significant differences in gut microbiome composition between the individuals after 20 days (permutational multivariate analysis of variance [PERMANOVA] $P < 0.05$; Figs. 1C and D), suggesting a high inter-individual diversity in gut microbiomes between the seven siblings even under the same rearing environments.

Variations in the relative abundance of OTUs across a lifetime. We found nine distinct dynamic patterns (clusters) in the relative abundance of OTUs (>0.1% abundance) across lifetimes in the seven siblings, based on the Silhouette index calculation (Figs. 2 and Extended Data Fig. 3). Clusters_1 and 4 contained OTUs with a relatively high appearance frequency and constantly high abundance throughout most of their lifetime. Cluster_2 contained OTUs with two transient peaks in both early and late lifetimes. Cluster_3 contained OTUs detected immediately after birth, and almost disappeared in the latter lifetime. Cluster_5 contained OTUs with the highest abundance in the first half of the latter half of life, whereas Cluster_6 contained OTUs with higher abundance in the latter half of the first half of life. Cluster_7 contained OTUs with a transient peak in early age and a slight increase in late age. Cluster_8 contained OTUs with two transient peaks in the early (~50 days) and middle lifetimes (~500 days), with a relatively lower abundance in the latter half of the first half of the lifetime. Cluster_9 contained OTUs that transiently increased only at the early lifetime, which was limited to one mouse (M3). For the transient OTUs in the early lifetime, OTUs in Clusters_2, 4, 5, 7, and 9 increased after the earliest OTUs in Cluster_3 appeared (Extended Data Fig. 4).

Life-core and transient OTUs/species across a lifetime. Histograms of the number of OTUs (≥0.1% abundance in at least one sample) along the appearance frequency showed a bimodal distribution in all samples of the seven siblings (Fig. 3A). We then defined OTUs detected in >80% and <20% of all samples from each mouse as "life-core" and "transient" OTUs, respectively. We found 74 non-redundant life-core OTUs (varying from 48 to 60 in seven siblings), of which 38 (minimum life-core OTUs, 51%) were common in all mice and belonged to Clusters_1 and/or 4, and seven (9.5%) were specific to individuals (Table S2). In contrast, 989 non-redundant transient OTUs (varying from 317

126 to 448 in seven siblings) were found in the samples and included only six (0.6%) common OTUs
127 belonging to Clusters_2, 3, and 5, and 394 (39.8%) were specific to individuals (Table S3). Taxonomic
128 assignment revealed that all life-core OTUs belonged to the four major phyla of the gut microbiome,
129 of which 52 (70%) and 31 (82%) were assigned to Bacteroidetes in the core and minimum life-core
130 OTUs, respectively. In contrast, the transient OTUs belonged to more than nine phyla, of which 816
131 (83%) were assigned to Firmicutes (Fig. 3B). In addition, life-core OTUs had a relatively high
132 abundance compared to transient OTUs (Extended Data Fig. 5).
133
134 **Correlation of alpha diversity with the lifespan of the host.** As the seven siblings had different
135 lifespans ranging from 832 to 1,049 days under the same rearing environments (Table S1), we explored
136 the correlation between gut microbiome structure and their lifespans. To this end, we developed a
137 method to identify and assess microbial variables correlated with lifespan, based on Spearman's
138 correlation coefficient (Extended Data Fig. 6, see Methods). The analysis revealed strong correlations
139 between lifespan and α-diversity indices (OTU#, Shannon's index) in samples at certain ages
140 (Extended Data Fig. 7): significant positive correlations with the indices at ages from 500 to 700 days,
141 and significant negative correlations with the indices at ages after 800 days.
142
143 **Correlation of OTU abundance with the lifespan of the host.** Using the same method, we also
144 found that 17 OTUs in samples at certain ages were significantly correlated in abundance with lifespan
145 (Fig. 4). Seven OTUs (OTU00012, OTU00013, OTU00028, OTU00035, OTU00037, OTU00055, and
146 OTU00105) were negatively correlated in abundance with late age (late period of the lifetime, after
147 800 days); two OTUs (OTU00006 and OTU00076) were positively correlated in abundance with
148 middle age (middle period of the lifetime, from 100 to 600 days) and negatively correlated with late
149 age; two OTUs (OTU00041 and OTU01676) were positively correlated in abundance with late age;
150 four OTUs (OTU00023, OTU00045, OTU00063, and OTU00069) were positively correlated in
151 abundance with middle age; and two OTUs (OTU00019 and OTU00033) were negatively correlated
152 in abundance with middle age.
153
154 **OTUs that correlated with life events.** We also investigated OTUs associated with several life events,
155 such as pregnancy, body weight, tumorigenesis, and cohousing, and compared them with the 17
156 lifespan-associated OTUs.
157 Three mice (M3, M7, and Mo) underwent pregnancy/delivery during the experiment.
158 Comparison of UniFrac distances between samples 20 days before pregnancy, during pregnancy, and
159 after delivery in these mice revealed significant differences in unweighted UniFrac distance between
160 any pair of three samples and in weighted UiFrac distance between before and during pregnancy
161 samples and between before and after delivery samples (PERMANOVA, $P < 0.05$; Extended Data

Fig.8A). The number of OTUs was not significantly different between the samples; however, Shannon's index was significantly increased in samples during pregnancy and after delivery compared to samples before pregnancy (Extended Data Fig. 8B). The analysis also revealed 59 OTUs with significant changes in abundance between samples (Table S4). These included four lifespan-associated OTUs (OTU00023, OTU00033, OTU00063, and OTU00076), which were significantly different before and after delivery.

We found that OTUs significantly correlated with body weight in samples collected from later stages of life from day 555 to just before death, and identified 27 OTUs significantly correlated in abundance with body weight ($P < 0.05$, average rho >0.3; Extended Data Fig. 9). Of these, two OTUs (OTU00006 and OTU00045) were lifespan-associated OTUs; OTU00006 was negatively correlated whereas OTU00045 was positively correlated with body weight.

We observed tumors in five mice (M2, 6, 7, 8, and Mo) by immediate autopsy of the dead mice. UniFrac distance analysis of samples 30 days before death revealed that the gut microbiome significantly differed between samples with and without tumors (Extended Data Fig. 10A). Both the number of OTUs and Shannon's index were higher in the tumor samples than in the non-tumor samples (Extended Data Fig. 10B). We also identified 32 and 33 OTUs that were significantly enriched and depleted, respectively, in tumor samples compared to non-tumor samples (Table S5). Of these, five (OTU00006, OTU00012, OTU00013, OTU00035, and OTU00105) and two OTUs (OTU00041 and OTU00055) were lifespan-associated OTUs.

During the experiments, 10 mice (eight siblings and parents) were cohoused with different combinations of individuals in different frequencies and periods after initially cohousing all mice together for 51 days after birth (Extended Data Fig. 11). We divided the samples after 20 days into those with and without cohousing and compared their UniFrac distances. The results revealed that both weighted and unweighted UniFrac distances were significantly lower in housed samples than in non-housed samples (Extended Data Fig. 12).

Overlap between the lifespan- and life events-associated OTUs. As mentioned above, we identified 17 lifespan-associated OTUs, 59 pregnancy-associated OTUs, 27 body weight-associated OTUs, and 65 tumor-associated OTUs. These 168 OTUs were clustered to generate 127 OTUs specific to either of the four categories, and 29 and 6 OTUs overlapped with 2 and 3 host factors, respectively (Table. S6). Of the 17 lifespan-associated OTUs, 7 (41%) overlapped with tumors, four with pregnancy, and two with body weight.

Discussion

This is a comprehensive time-course study that elucidates the development of the gut microbiome over the lifespan of cognate SPF mice. The relationship between the gut microbiome and host aging has

been well recognized; however, it is mostly based on the comparative analysis of gut microbiomes between individuals of various ages with different dietary habits, lifestyles, and genetic backgrounds. In this study, we used sibling mice and longitudinally monitored changes in the gut microbiome of individuals from birth to death for approximately three years. Even though the mice were bred in a controlled environment, we eventually observed phenotypic diversity between individuals, accompanied by the development of the gut microbiome. As C57BL/6J mice were designed as an inbred line and have common genetic backgrounds, these diverse individual differences are likely caused by stochastic environmental factors.

In this study, we found, for the first time, a tendency for increased diversity of the gut microbiome before death by observing the variation in gut bacteria over the course of a lifetime in mice (Extended Data Fig. 2). Age-related gut microbiome transitions have been observed in several cohort studies; however, changes in gut microbial diversity in adults have been controversial[19]. Many studies in developed countries have suggested that the microbiota is relatively stable throughout adulthood, and that aging induces significant shifts in gut microbiome composition and function that are associated with a decline in diversity[15,20]. In contrast, another study targeting hunter-gatherers in Hadza reported an increase in microbial diversity in the older adult population[21]. The increase in diversity found in this study is consistent with the Hadza study. The older adults in the industrialized cohort might have been affected by a medical treatment such as antibiotics, whereas the increased diversity seen in mice in our study and the Hadza study could be due to the absence of the effect of medications. In the older adult population, a drop in immune fitness has been reported, accompanied by impaired hematopoiesis, higher susceptibility to infections, and reduced responses to vaccination[22–28]. Therefore, the increase in gut microbial diversity found in this study and the Hadza study suggests a relationship with immune weakening due to aging.

In the present study, the analysis of variation patterns of OTU abundance revealed nine distinct dynamic patterns of OTU abundance across the lifetime of seven siblings (Fig. 2). At approximately day 500–600, we also observed a significant change in the dynamics of OTUs in clusters 5 and 6. OTUs in cluster 5 decreased after day 500–600 whereas the dynamics of the ones in cluster 6 increased in the latter half of life. These results suggest that some mode changes related to the dynamics of the gut microbiota may have occurred around day 500–600; however, it is unclear whether this is due to changes in host homeostasis or the ecological balance of the gut microbiota. Additionally. our results suggest that some microbes persist for almost a lifetime in high abundance (Fig. 3); however, Caporaso et al. have suggested, based on two individual human time series analyses, that no core temporal microbiome exists at high abundance[29]. This discrepancy may be because the mice in our study were raised in a stable environment and were not affected by medication. Moreover, the bimodal distribution indicated that OTUs can be largely divided into “life-core” and “transient” OTUs. “Life-core” OTUs were largely dominated by Bacteroidetes whereas transient OTUs were

234 mostly composed of Firmicutes. These results are consistent with a study by Faith et al. reporting that
235 Bacteroidetes and Actinobacteria are significantly more stable over time in humans[34]. Bacteroidetes
236 and Firmicutes are both dominant phyla in gut microbiomes; however, our results indicated differences
237 in their persistence throughout life. The Bacteroidetes group tends to persist for a long time whereas
238 most of the Firmicutes group, although high in abundance, may be unable to persist. A previous report
239 based on fluorescent in situ hybridization imaging technology showed that Bacteroidetes are mostly
240 observed near the intestinal wall, whereas Firmicutes are separated from the gut wall in the mouse
241 intestinal tract[30]. Therefore, the settling of Bacteroidetes in the gut wall may allow them to persist in
242 the host. In addition to their location in the gut, Firmicutes have been proposed to be more effective
243 in extracting energy from food than Bacteroidetes, thereby promoting more efficient absorption of
244 calories and subsequent weight gain[31,32]. MacFarlane et al. reported that Bacteroidetes mainly produce
245 acetate and propionate whereas Firmicutes produces more butyrate[33]. These differences in the
246 metabolic capacity of Firmicutes and Bacteroidetes might also affect their persistence.
247 In the present study, we developed an original method to determine the dynamic relationship
248 between the gut microbiome and lifespan at various times in life: a positive correlation in middle age
249 (day 500–700) and a negative correlation in old age (after day 800) (Extended Data Fig.7). As many
250 diseases have been reported to lower the diversity of gut bacteria[35–37], it is often discussed that higher
251 diversity is related to a healthier life. However, in this study, the average α-diversity throughout life
252 was not strongly correlated with the lifespan (Extended Data Fig. 7). Although higher diversity was
253 correlated with a longer lifespan only in the middle period of life (day500~600), an opposite
254 correlation was found in old age (after day 800). Moreover, the correlation between abundance and
255 lifespan of OTUs before day 400 tended to be weaker than that in later life. We further found 17 OTUs
256 that were strongly associated with lifespan, most of which were life-core OTUs (Fig. 4), although this
257 correlation was altered or even reversed for many OTUs around day 500–600. Among the 17 lifespan-
258 associated OTUs, Lactobacillus was negatively correlated with the middle period of life and showed
259 a significant positive correlation later in life (after day 700). The abundance of Lactobacillus has been
260 reported to decrease with age. Furthermore, an increase in Lactobacillus has been reported to be
261 associated with lifespan elongation under limited calorie conditions in mice[10]. In our study, a
262 consistent tendency was observed in aged mice but not in young mice. We also found that OTU33,
263 which was closest to *B. vulgatus* (93.3%), showed a positive correlation with lifespan in later life but
264 a negative correlation in early life (before day 500). *B. vulgatus* was reported to have a significantly
265 higher abundance in village communities in Korea, where longevity is common[38]. This correlation
266 between a higher abundance of *B. vulgatus* and longevity is consistent with our results in later life but
267 not in early life. Additionally, immunosuppressive drug rapamycin and the anti-diabetic drug
268 metformin, have recently been reported to extend the lifespan of mice related with gut microbiome[3,39].
269 In our study, the lifespan-associated OTUs included the genera Bacteroides and

Lactobacillus/Alistipes, which are known to be affected by rapamycin and metformin in mice, respectively. The change in correlation pattern with age suggest the possibility that the previously reported relationship between microbes and lifespan can also be a correlation found only at certain times in lifetimes.

In addition, some lifespan-associated OTUs were associated with pregnancy, body weight, and tumor development (Table S6). OTU00033 (*B. vulgatus* 93.02%) decreased after pregnancy and was negatively associated with longevity in young mice whereas OTU00023 (C. fastidious 83.44%), OTU00063 (*P. capillosus* 90.77%), and OTU00076 (*E. coprostanoligenes* 90.29%) increased after pregnancy, and were positively associated with longevity in young mice. Therefore, diversity increased with pregnancy, and higher diversity in youth was associated with longevity. Despite the limited number of mice in this study, these results indirectly suggest that pregnancy at a young age might be associated with longevity. Moreover, OTU00006 (*B. caecigallinarum* 90.16%) was negatively correlated with both body weight and longevity in old mice whereas OTU00045 (*P. timonensis* 87.9%) was positively correlated with both body weight and longevity (Table S6). These results indirectly suggest that weight gain in old age might be associated with longevity. Five OTUs (OTU00006, OTU00012, OTU00013, OTU00035, and OTU00105) enriched in tumor-developed mice were negatively associated with longevity in aged mice (Table S6). Additionally, diversity increased with tumor development, and higher diversity in aged mice was negatively associated with longevity. These results are consistent with the obvious conclusion that the absence of tumors in old age is associated with longevity.

In this study, for the first time, we characterized the life-core microbiome and showed that the temporal dynamics of some life-core OTUs are significantly correlated with lifespan. This study strongly suggests a close relationship between bacterial dynamics and lifespan. Further investigation of host immune changes or bacterial functional interactions will help clarify the mechanism underlying the temporal dynamics of diversity and bacterial abundance observed in this study.

Methods

Fecal collection in mouse experiments. Two SPF C57BL/6J mice were maintained and bred under specific pathogen-free conditions at RIKEN Center for Integrative Medical Sciences Animal Facility or conventional facility at Yokohama City University. (Kanagawa, Japan). Male and female offspring were separated after weaning for 50-51 days. The mouse cages were replaced primarily to control reproduction. The starting point of this study was the birth of the second generation of SPF mice. Each mouse in each group was recognized using ear punches. Nine offspring were born. All mice were kept in a room at 23 ± 2°C, 50 ± 10% relative humidity, on a 12-h light/dark cycle. The animals were housed in cages (Extended Data Fig. 11) with wood shavings and fed (CE-2, CLEA Japan, Inc.) and

305 watered ad libitum. Male mouse (M1) was fed Oriental CMF (Oriental Yeast, Tokyo) from day 462-
306 559 for breeding. One of the nice offspring died at 6 days of age and was therefore excluded from the
307 analysis (M9). Another mouse (M6) was excluded from the analysis of the association of the gut
308 microbiome with lifespan because it died during retention during sample collection due to debilitation.
309 Mouse feces were collected, snap-frozen, and stored at −80 °C. All animal experiments were approved
310 by the Institutional Animal Care and Use Committees of RIKEN Yokohama Branch and Yokohama
311 City University.
312
313 **Autopsies of dead mice.** Dead mice were immediately stored in a freezer (−20 °C). After thawing,
314 they were dissected by a surgeon researcher, who visually checked the left and right kidneys, spleen,
315 lungs, heart, cervical lymph nodes, ovaries, prostate, and liver for the presence of tumors.
316
317 **DNA extraction.** Bacterial genomic DNA was extracted from mouse feces using enzymatic lysis
318 method. Frozen fecal pellets were thawed and suspended in 1 mL of TE10 (10 mM Tris-HCl, 10 mM
319 EDTA) buffer containing RNaseA (final concentration of 100 μg/mL; Nippon Gene, Tokyo, Japan).
320 Lysozyme (Sigma-Aldrich; St. Louis, MO, USA) was added at a final concentration of 15 mg/mL,
321 and the suspension was incubated for 1 h at 37 °C with gentle mixing. Purified achromopeptidase
322 (Wako Pure Chemical, Osaka, Japan) was added at a final concentration of 2000 units/mL, and the
323 suspension was further incubated for 30 min at 37 °C. Sodium dodecyl sulfate (final concentration, 1
324 mg/mL) and proteinase K (final concentration, 1 mg/mL; MERCK Group Japan, Tokyo, Japan) were
325 added to the sample, and the mixture was incubated for 1 h at 55 °C. DNA was extracted with
326 phenol/chloroform/isoamyl alcohol (25:24:1), precipitated with isopropanol and 3 M sodium acetate,
327 washed with 75% ethanol, and resuspended in 200 μL of TE buffer. DNA was purified with a 20%
328 PEG solution (PEG6000 in 2.5 M NaCl), pelleted by centrifugation, rinsed with 75% ethanol, and
329 dissolved in TE buffer.
330
331 **16S rRNA gene amplicon sequencing.** In this study, we analyzed a total of 51.4 million (51,377,124
332 reads) high-quality reads of the 16S rRNA gene V1-2 region from eight siblings and the parents
333 (Supplementary Table 1). The isolated DNA (40 ng) was used for PCR amplification of the V1–V2
334 hypervariable regions of the 16S rRNA gene using the universal primers 27Fmod (5′-
335 AATGATACGGCGACCACCGAGATCTACACxxxxxxxxACACTCTTTCCCTACACGACGCTC
336 TTCCGATCTagrgtttgatymtggctcag-3′) and 338R (5′-
337 CAAGCAGAAGACGGCATACGAGATxxxxxxxxGTGACTGGAGTTCAGACGTGTGCTCTTCC
338 GATCTtgctgcctcccgtaggagt-3′), containing the Illumina Nextera adapter sequence and a unique 8-bp
339 index sequence for each sample. Thermal cycling was performed on a 9700 PCR system (Life
340 Technologies, Carlsbad, CA, USA) using Ex Taq polymerase (Takara Bio, Tokyo, Japan) with the

following cycling conditions: initial denaturation at 96 °C for 2 min; 25 cycles of denaturation at 96 °C for 30 s, annealing at 55° C for 45 s, and extension at 72 °C for 1 min; and final extension at 72 °C. All amplicons were purified using AMPure XP magnetic purification beads (Beckman Coulter, Brea, CA, USA) and quantified using the Quant-iT PicoGreen dsDNA Assay kit (Life Technologies). An equal amount of each PCR amplicon was mixed and subjected to sequencing with MiSeq (Illumina) using the MiSeq Reagent Kit v3 (600 cycles) according to the manufacturer's instructions.

Data analysis. After demultiplexing the 16S sequence reads based on a sample-specific index, paired-end reads were joined using the fastq-join program. Reads with average quality values <25 and inexact matches to the universal primer sequences were filtered; 3,000 reads that passed the quality filter were randomly selected from each sample and subjected to downstream analysis. The selected reads of all the samples were first sorted by the frequency of redundant sequences and grouped into operational taxonomic units (OTUs) using UCLUST (https://www.drive5.com/) with a sequence identity threshold of 97%. The taxonomic assignment of each operational taxonomic unit was determined by similarity searching against the Ribosomal Database Project and NCBI genome database using the GLSEARCH program.

Temporal dynamics clusters analysis.

Temporal dynamics clusters were calculated on the time-course data of OTU abundances. Bray-Curtis distance between the OTU abundances were calculated and hierarchically clustered by 'hclust' function R software program (v4.1.1) with 'ward.D2' method. The optimal number of clusters were calculated by 'find_k' function from R library 'dendextend'.

Statistical analysis. All statistical analyses were conducted with the R software program (v4.1.1). Wilcoxon rank sum test was used for comparison of alpha diversities and the proportion of gut microbiome at the phylum, genus, and OTU levels. PERMANOVA was used to compare the gut microbiome structure among groups based on both weighted and unweighted UniFrac distance. P values were corrected for multiple testing using the Benjamin–Hochberg method as appropriate.

Correlation analysis of the gut microbiome with lifespan. In the correlation analysis of the gut microbiome structure and lifespan of the seven siblings, the variables (abundance of the bacteria/OTUs and diversity indices of communities) that were significantly correlated with lifespan were determined using the following five steps (Extended Data Fig. 6): (1) we calculated Spearman's correlation coefficients between lifespan and the variables of samples at each time point lifetime (days); (2) we calculated the moving average of the correlation coefficients of samples as it shifted every 50 days throughout the lifetime (see the trend of the entire period by taking the average of 50 days in shifts); (3) we developed a time series in which the sampling time is completely randomly switched, and the

moving average of the correlation was calculated in the same way; (4) we defined the range of possible values of the moving average of the correlation coefficients of the random time series (not strongly correlated with life expectancy at a particular time) calculated in step 3 in terms of the average value and the 3σ range; and (5) finally, if the actual time series showed a moving average value that clearly deviates from the range defined in step 4, we considered it significant.

Data availability

The 16S rRNA V1–V2 region sequences analyzed in the current study were deposited in DDBJ/GenBank/EMBL under accession XXXXXXXX.

Acknowledgements

We thank K. Kaida, C. Shindo, J. Noack, M. Takagi, and M. Tanokura (RIKEN) for their technical support.

This work was supported by JSPS KAKENHI (Grant Number 21409803) and a RIKEN Integrated Symbiology grant (to M.H. and W.S.).

Author contributions

Experimental design, L.T. and W.S.; sampling and experiment, L. T., E.W., and T.U.; 16S rRNA sequencing, R.K., Y.O, Y.K., H.M.; Statistical analysis, L.T.; Writing—Original Draft, L.T.; Writing—Review & Editing, W.S., M.U., and M.H.; Supervision, W.S. and M.H.; Funding Acquisition, L.T., W.S., M.H.

Competing interests

The authors declare no competing interests.

Figure legends

Fig. 1. Principle coordinate analysis (PCoA) based on UniFrac distance.

A, PCoA of seven mice from day 0 to day 1044 of life-based on the weighted UniFrac distance. The color corresponds to the day after birth. **B**, PCoA of seven mice from day 0 to day 1044 based on the unweighted UniFrac distance. The color corresponds to the day after birth. **C**, PCoA of seven mice from day 20 to day 1044 based on the weighted UniFrac distance. Color corresponds to an individual mouse. **D**, PCoA of seven mice from day 20 to day 1044 based on the unweighted UniFrac distance. The color corresponds to an individual mouse.

Fig. 2. The nine clusters of temporal operational taxonomic unit (OTU) dynamics.

The average relative abundance of the OTUs included in each of the nine temporal dynamic clusters is shown. Temporal dynamics clusters were optimally determined based on average silhouette width (See Methods).

Fig. 3. Life-core and transient microbiome.

The upper figures are histograms of the observed frequency of the operational taxonomic units (OTUs) (maximum relative abundance $\geq$ 0.1%). The observed frequency was calculated by dividing the number of times when an abundance of more than 0 reads was observed by the total number of observed times. The bar graphs below indicate the phylum-level composition of the OTUs in each bin.

Fig. 4. Seventeen operational taxonomic units (OTUs) are significantly correlated with lifespan in mice.

Spearman's correlation coefficients between the abundance of 17 lifespan-associated OTU and lifespans are shown. The orange dots indicate Spearman's correlation coefficient at each time point. The blue dots indicate the simple moving average of the coefficients over 50 time points. The yellow mesh indicates the confidence interval (3σ).

References

1. Gordon, H. A., Bruckner-Kardoss, E. & Wostmann, B. S. Aging in germ-free mice: life tables and lesions observed at natural death. *J. Gerontol.* **21**, 380–387 (1966).

2. He, B. *et al.* Antibiotic-modulated microbiome suppresses lethal inflammation and prolongs lifespan in Treg-deficient mice. *Microbiome* **7**, 145 (2019).

3. Bitto, A. *et al.* Transient rapamycin treatment can increase lifespan and healthspan in middle-aged mice. *Elife* **5**, (2016).

4. Bárcena, C. *et al.* Healthspan and lifespan extension by fecal microbiota transplantation into progeroid mice. *Nat. Med.* **25**, 1234–1242 (2019).

5. Matsumoto, M., Kurihara, S., Kibe, R., Ashida, H. & Benno, Y. Longevity in mice is promoted by probiotic-induced suppression of colonic senescence dependent on upregulation of gut bacterial polyamine production. *PLoS One* **6**, e23652 (2011).

6. Cerro, E. D.-D. *et al.* Daily ingestion of Akkermansia muciniphila for one month promotes healthy aging and increases lifespan in old female mice. *Biogerontology* **23**, 35–52 (2022).

7. Fontana, L., Partridge, L. & Longo, V. D. Extending Healthy Life Span—From Yeast to Humans. *Science* (2010) doi:10.1126/science.1172539.

8. Rizza, W., Veronese, N. & Fontana, L. What are the roles of calorie restriction and diet quality in promoting healthy longevity? *Ageing Res. Rev.* **13**, 38–45 (2014).

447 9. Mercken, E. M., Carboneau, B. A., Krzysik-Walker, S. M. & de Cabo, R. Of mice and men: the
448 benefits of caloric restriction, exercise, and mimetics. *Ageing Res. Rev.* **11**, 390–398 (2012).
449 10. Zhang, C. *et al.* Structural modulation of gut microbiota in life-long calorie-restricted mice. *Nat.*
450 *Commun.* **4**, 2163 (2013).
451 11. Yatsunenko, T. *et al.* Human gut microbiome viewed across age and geography. *Nature* **486**,
452 222–227 (2012).
453 12. Odamaki, T. *et al.* Age-related changes in gut microbiota composition from newborn to
454 centenarian: a cross-sectional study. *BMC Microbiol.* **16**, 90 (2016).
455 13. Claesson, M. J. *et al.* Composition, variability, and temporal stability of the intestinal microbiota
456 of the elderly. *Proc. Natl. Acad. Sci. U. S. A.* **108 Suppl 1**, 4586–4591 (2011).
457 14. Claesson, M. J. *et al.* Gut microbiota composition correlates with diet and health in the elderly.
458 *Nature* **488**, 178–184 (2012).
459 15. Biagi, E. *et al.* Gut Microbiota and Extreme Longevity. *Curr. Biol.* **26**, 1480–1485 (2016).
460 16. Wu, L. *et al.* A Cross-Sectional Study of Compositional and Functional Profiles of Gut
461 Microbiota in Sardinian Centenarians. *mSystems* **4**, (2019).
462 17. Rampelli, S. *et al.* Shotgun Metagenomics of Gut Microbiota in Humans with up to Extreme
463 Longevity and the Increasing Role of Xenobiotic Degradation. *mSystems* **5**, (2020).
464 18. Si, J. *et al.* Long-term life history predicts current gut microbiome in a population-based cohort

study. *Nat Aging* (2022) doi:10.1038/s43587-022-00286-w.

19. Martino, C. *et al.* Microbiota succession throughout life from the cradle to the grave. *Nat. Rev. Microbiol.* (2022) doi:10.1038/s41579-022-00768-z.

20. Badal, V. D. *et al.* The gut microbiome, aging, and longevity: A systematic review. *Nutrients* **12**, 3759 (2020).

21. Schnorr, S. L. *et al.* Gut microbiome of the Hadza hunter-gatherers. *Nat. Commun.* **5**, 3654 (2014).

22. Bosco, N. & Noti, M. The aging gut microbiome and its impact on host immunity. *Genes Immun.* **22**, 289–303 (2021).

23. Broxmeyer, H. E. *et al.* Fate of hematopoiesis during aging. What do we really know, and what are its implications? *Stem Cell Rev Rep* **16**, 1020–1048 (2020).

24. Kovtonyuk, L. V., Fritsch, K., Feng, X., Manz, M. G. & Takizawa, H. Inflamm-aging of hematopoiesis, hematopoietic stem cells, and the bone marrow microenvironment. *Front. Immunol.* **7**, 502 (2016).

25. Goronzy, J. J. & Weyand, C. M. Understanding immunosenescence to improve responses to vaccines. *Nat. Immunol.* **14**, 428–436 (2013).

26. Thomas, R., Wang, W. & Su, D.-M. Contributions of age-related thymic involution to immunosenescence and inflammaging. *Immun. Ageing* **17**, 2 (2020).

27. Cianci, R. *et al.* The interplay between immunosenescence and Microbiota in the efficacy of

vaccines. *Vaccines (Basel)* **8**, 636 (2020).

28. Amsterdam, D. & Ostrov, B. E. The impact of the microbiome on immunosenescence. *Immunol. Invest.* **47**, 801–811 (2018).

29. Caporaso, J. G. *et al.* Moving pictures of the human microbiome. *Genome Biol.* **12**, R50 (2011).

30. Earle, K. A. *et al.* Quantitative Imaging of Gut Microbiota Spatial Organization. *Cell Host Microbe* **18**, 478–488 (2015).

31. Krajmalnik-Brown, R., Ilhan, Z.-E., Kang, D.-W. & DiBaise, J. K. Effects of gut microbes on nutrient absorption and energy regulation. *Nutr. Clin. Pract.* **27**, 201–214 (2012).

32. Magne, F. *et al.* The Firmicutes/Bacteroidetes Ratio: A Relevant Marker of Gut Dysbiosis in Obese Patients? *Nutrients* **12**, (2020).

33. Fei, N. & Zhao, L. An opportunistic pathogen isolated from the gut of an obese human causes obesity in germfree mice. *ISME J.* **7**, 880–884 (2013).

34. Faith, J. J. *et al.* The Long-Term Stability of the Human Gut Microbiota. *Science* (2013) doi:10.1126/science.1237439.

35. Kriss, M., Hazleton, K. Z., Nusbacher, N. M., Martin, C. G. & Lozupone, C. A. Low diversity gut microbiota dysbiosis: drivers, functional implications and recovery. *Curr. Opin. Microbiol.* **44**, 34–40 (2018).

36. Brown, K., DeCoffe, D., Molcan, E. & Gibson, D. L. Diet-induced dysbiosis of the intestinal

501 microbiota and the effects on immunity and disease. *Nutrients* **4**, 1095–1119 (2012).

502 37. Mosca, A., Leclerc, M. & Hugot, J. P. Gut Microbiota Diversity and Human Diseases: Should

503 We Reintroduce Key Predators in Our Ecosystem? *Front. Microbiol.* **7**, 455 (2016).

504 38. Park, S.-H. *et al.* Comparative analysis of gut microbiota in elderly people of urbanized towns

505 and longevity villages. *BMC Microbiol.* **15**, 49 (2015).

506 39. Induri, S. N. R. *et al.* The Gut Microbiome, Metformin, and Aging. *Annu. Rev. Pharmacol.*

507 *Toxicol.* **62**, 85–108 (2022).

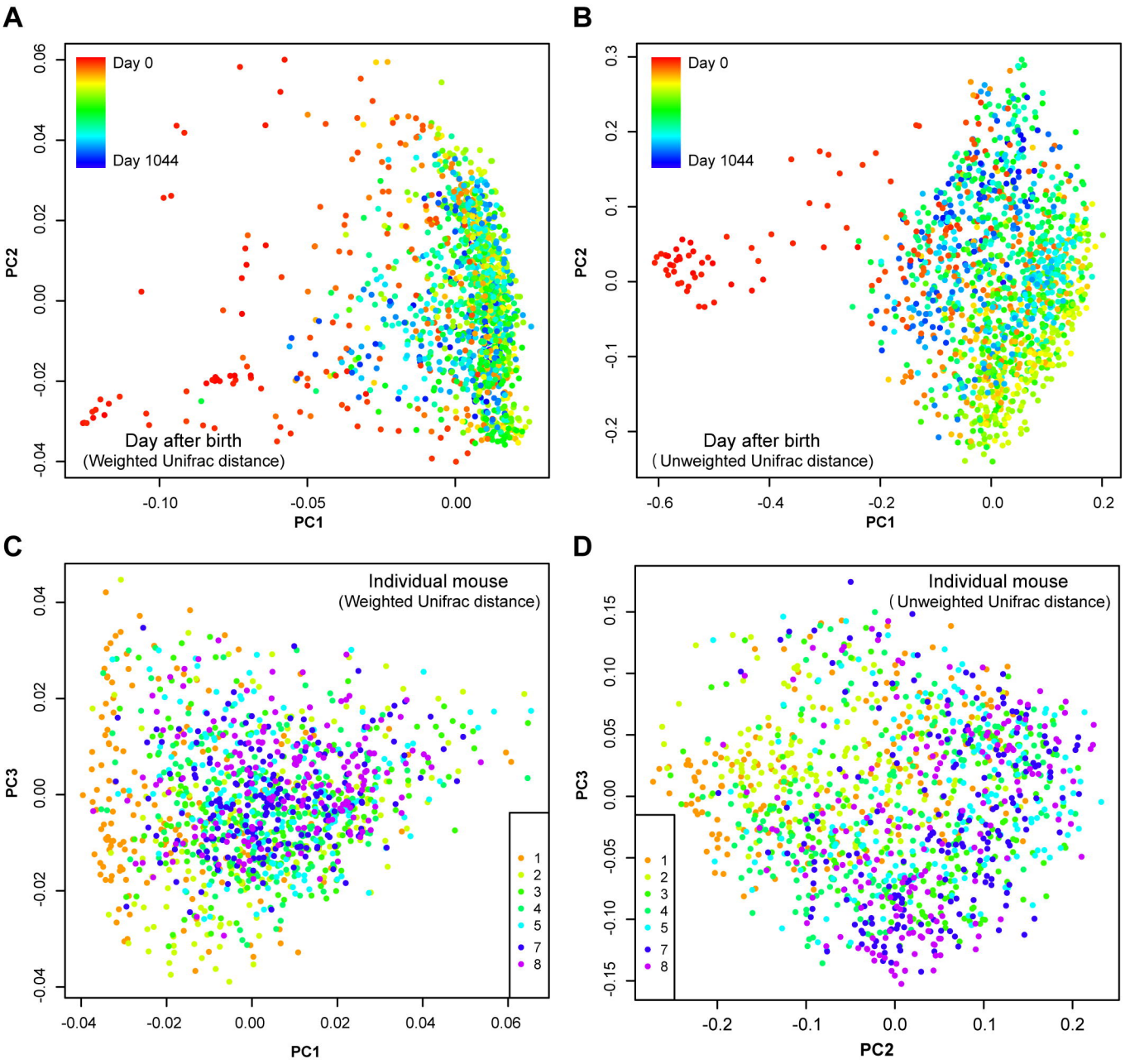
A
Day 0
Day 1044
Day after birth
(Weighted Unifrac distance)
PC1
PC2
B
Day 0
Day 1044
Day after birth
(Unweighted Unifrac distance)
PC1
PC2
C
Individual mouse
(Weighted Unifrac distance)
1
2
3
4
5
7
8
PC1
PC3
D
Individual mouse
(Unweighted Unifrac distance)
1
2
3
4
5
7
8
PC2
PC3

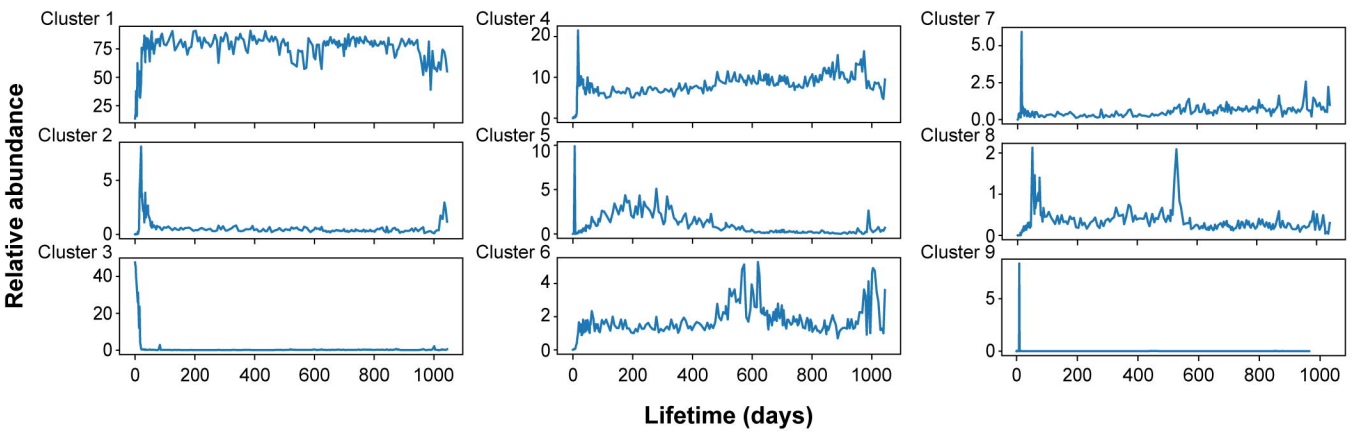
Cluster 1
Cluster 2
Cluster 3
Cluster 4
Cluster 5
Cluster 6
Cluster 7
Cluster 8
Cluster 9
Relative abundance
Lifetime (days)

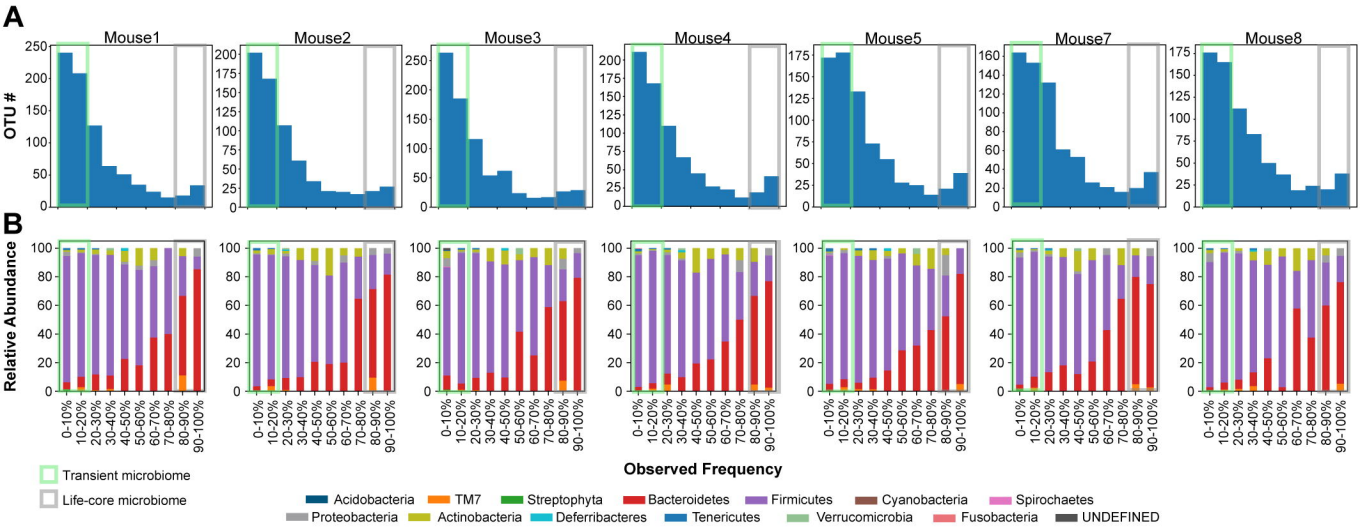
A
Mouse1
Mouse2
Mouse3
Mouse4
Mouse5
Mouse7
Mouse8
OTU #
B
Relative Abundance
0-10%
10-20%
20-30%
30-40%
40-50%
50-60%
60-70%
70-80%
80-90%
90-100%
Observed Frequency
Transient microbiome
Life-core microbiome
Acidobacteria
TM7
Streptophyta
Bacteroidetes
Firmicutes
Cyanobacteria
Spirochaetes
Proteobacteria
Actinobacteria
Deferribacteres
Tenericutes
Verrucomicrobia
Fusobacteria
UNDEFINED

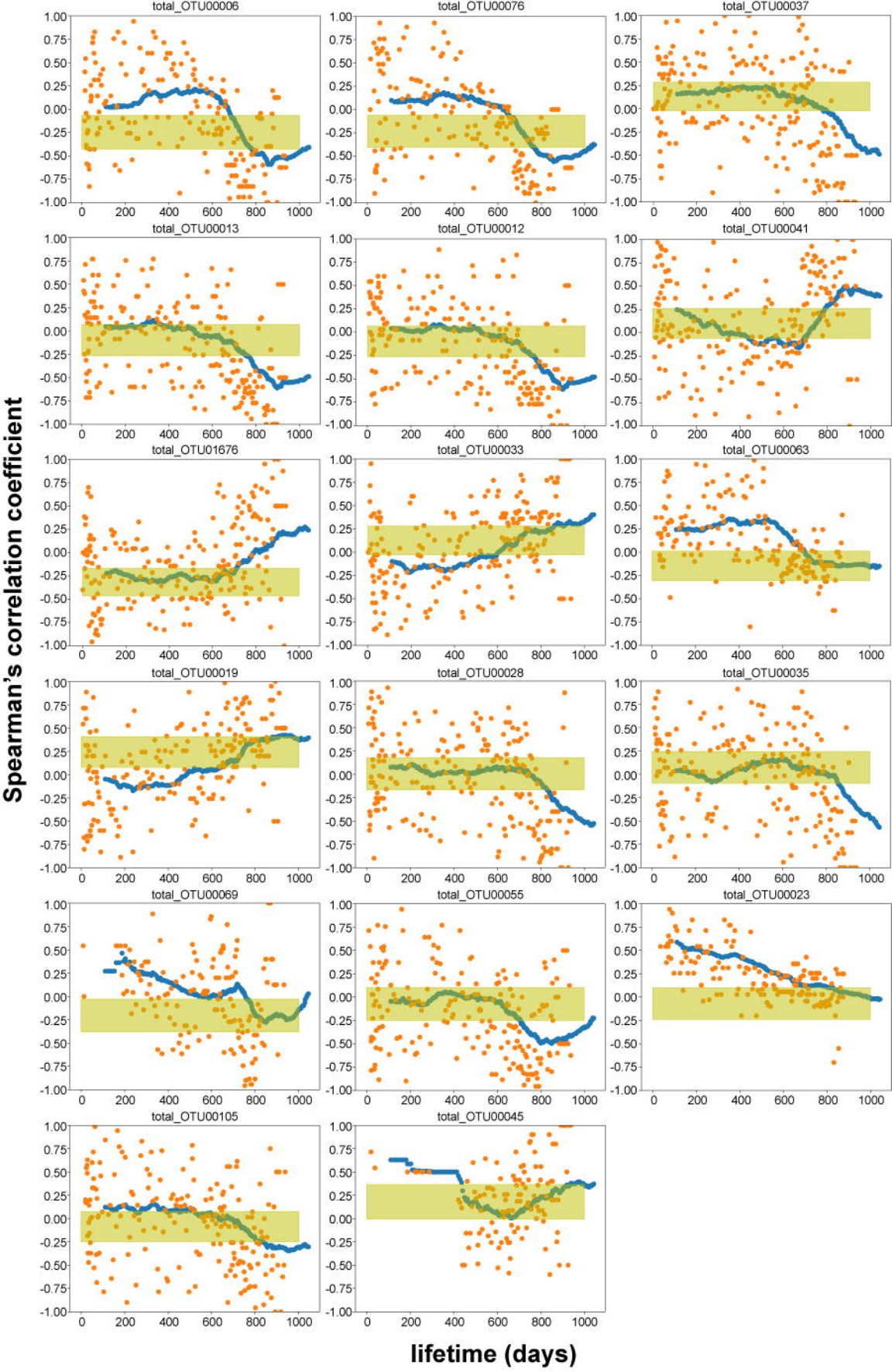
total_OTU00006
total_OTU00076
total_OTU00037
total_OTU00013
total_OTU00012
total_OTU00041
total_OTU01676
total_OTU00033
total_OTU00063
total_OTU00019
total_OTU00028
total_OTU00035
total_OTU00069
total_OTU00055
total_OTU00023
total_OTU00105
total_OTU00045
Spearman's correlation coefficient
lifetime (days)